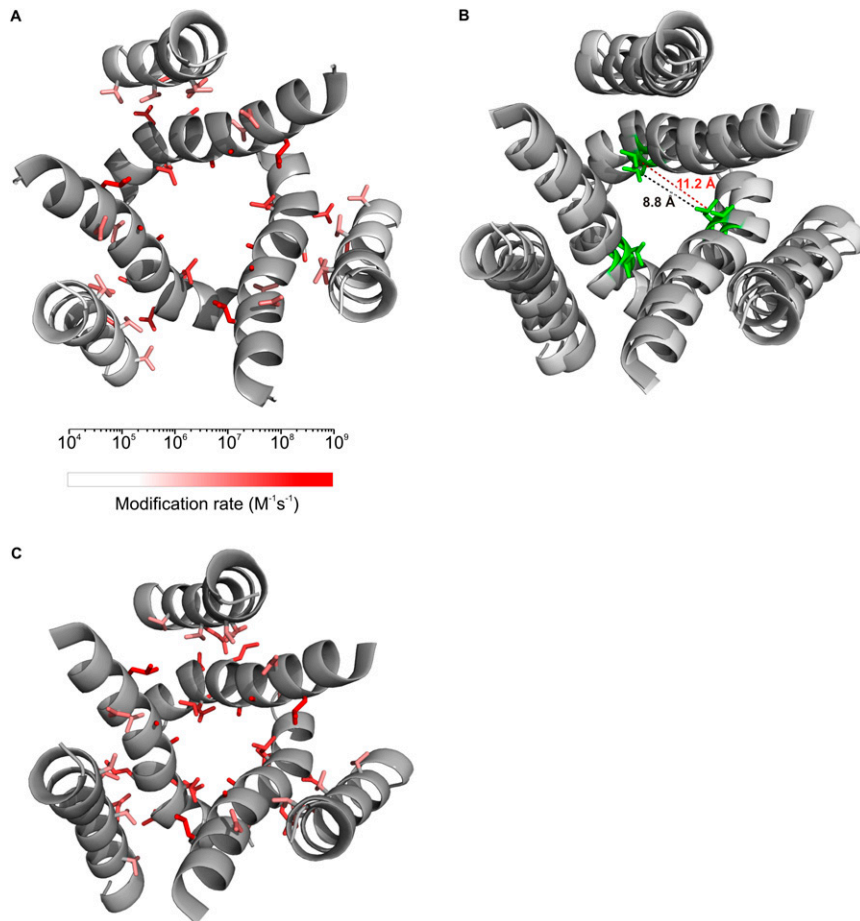


# Supporting Information

Heymann et al. 10.1073/pnas.1311071110



**Fig. S1.** Evaluation of the X-ray structure (Protein Data Bank ID code 4DW1) and our model of the ATP-bound zebra fish P2X4 (zfpP2X4) receptor against previous accessibility and bridging results. (A) Rates of Ag<sup>+</sup> modification of individual Cys residues (1, 2) mapped onto the transmembrane (TM) domain of the X-ray structure using the color scale shown. The TM domain is viewed from the external side of the membrane. (B) Compatibility of the X-ray structure (light gray) and model (dark gray) for ATP-bound zfpP2X4 receptors with the rat P2X2 (rP2X2) V343C inhibitory Cd<sup>2+</sup> bridge. Side chains of L351 (equivalent to 343 in rP2X2) are shown in green. Cβ-Cβ distances are shown in red for the X-ray structure and in black for the model. (C) Rates of Ag<sup>+</sup> modification of individual Cys residues mapped onto the TM domain of the open-state model using the color scale in A. The TM domains are viewed from the external side of the membrane.

1. Li M, Chang TH, Silberberg SD, Swartz KJ (2008) Gating the pore of P2X receptor channels. *Nat Neurosci* 11(8):883–887.
2. Li M, Kawate T, Silberberg SD, Swartz KJ (2010) Pore-opening mechanism in trimeric P2X receptor channels. *Nat Commun* 1:44.

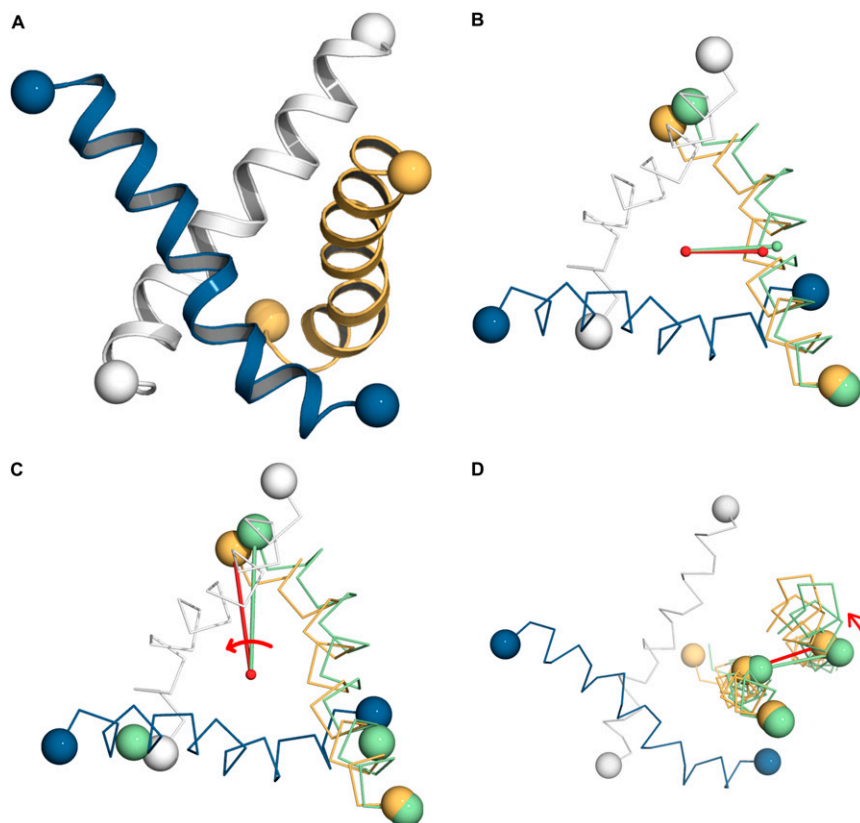


**Fig. S2.** Changes in the TM domain in the open-state model relative to the ATP-bound X-ray structure after superimposing the C $\alpha$  atoms of the I335 residues in the three subunits. (A) Oblique view into the pore lined by the TM2 helices of the open-state model. The same coloring scheme is used in subsequent panels. The N terminus (residue I335) and C terminus (residue I359) of TM2 are shown as spheres at the C $\alpha$  positions. (B) Decrease in distance between TM2 (as represented by the center of mass of its C $\alpha$  atoms) and the threefold axis from 8.3 Å (light green line and light green helix) in the ATP-bound zfp2X4 receptor to 7.0 Å (red line and gold helix) in the open-state model, as seen from the external side of the membrane. From the N terminus to the C terminus, the decrease in distance to the threefold axis becomes greater, contributing to tighter inter-TM2 packing and a greater decrease in pore radius toward the internal end of the open-state model. (C) Increase in the twist of the TM2 three-helix bundle by 10°, as measured by the change in rotation angle of the C terminus in the lateral plane and illustrated by the coloring scheme used as in B. The increased twist further tightens the inter-TM2 packing and reduces the pore radius toward the internal end of the open-state model. (D) Counterclockwise helical rotation of TM2 by 5° (as seen from the top), as illustrated by lines connecting G345 on TM2 and A44 on TM1 using the coloring scheme in B. This TM2 rotation places TM1 closer to the TM2 helix of a neighboring subunit.

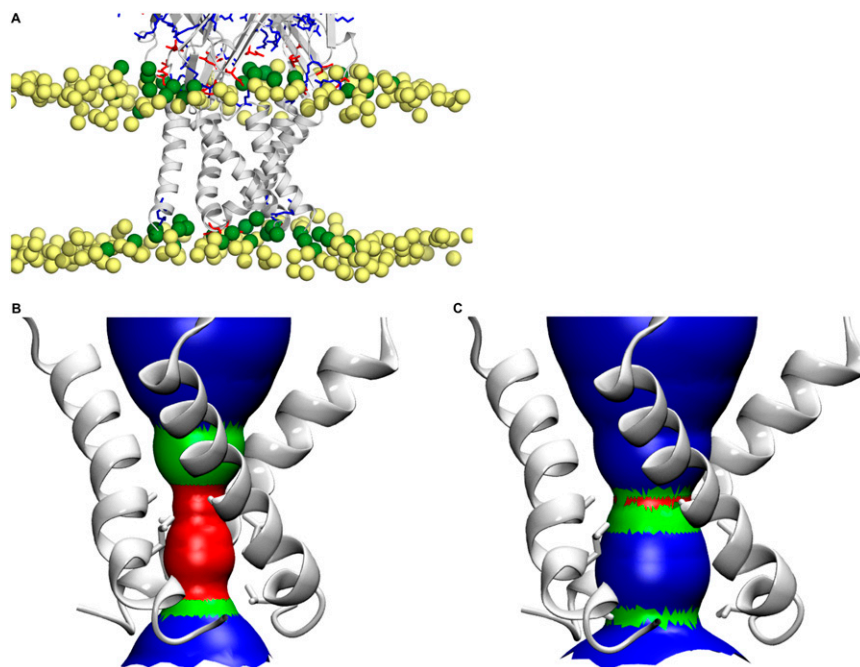


**Fig. S3.** Differences in hydrophobic mismatch and pore dimension between the open-state model and the ATP-bound X-ray structure. (A) Snapshot of the TM domain viewed parallel to the membrane at 30 ns in the molecular dynamics simulation of the open-state model. Blue and red sticks on the protein represent positively and negatively charged residues, respectively. Yellow spheres are phosphorous atoms of bulk lipid molecules, and green spheres are phosphorous atoms of lipids around the receptor. A similar simulation of the ATP-bound zfp2X4 X-ray structure showed a larger mismatch in membrane thickness between lipids that are adjacent to the receptor and bulk lipids (see Fig. 1F). The mismatch in membrane thickness (measured by the average distance separating the two layers of phosphorous atoms) between the adjacent and bulk lipids is 4.3 Å in that simulation. Here, in the simulation of the open-state model, the mismatch is reduced to 2.5 Å. (B) HOLE (1) image of the open-state model. Color code: red, radius <math>< 3.5 \text{ \AA}</math>; green, radius 3.5–4.5 Å; blue, radius >4.5 Å. TM2 helices are shown in gray; side chains of the pore-lining residues A347, L351, and V354 are shown as sticks. (C) HOLE image of the ATP-bound zfp2X4 X-ray structure.

1. Smart OS, Neduvellil JG, Wang X, Wallace BA, Sansom MS (1996) HOLE: A program for the analysis of the pore dimensions of ion channel structural models. *J Mol Graph* 14(6): 354–360, 376.

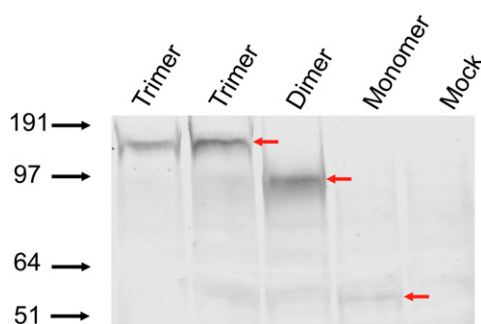


**Fig. S4.** Western blot from SDS/PAGE gel of concatenated and wild-type P2X2 receptors showing trimeric protein expression. Trimer lanes are from cells expressing concatenated trimers. The dimer lane is from cells expressing a concatenated dimer. The monomer lane is from cells expressing wild-type P2X2 receptor, and the mock lane is from untransfected cells. Red arrows mark the position of trimeric, dimeric, and monomeric receptor proteins. These experiments show the abundant presence of trimeric protein in cells expressing the concatenated trimer construct but do not rule out the presence of smaller quantities of dimeric or monomeric species. However, the control experiments in Fig. 4 led us to conclude that the potentiating H-C-C bridge must form within individual subunits.

**Table S1. Estimated EC<sub>50</sub> and Hill coefficients for ATP activation**

Construct	EC <sub>50</sub> , $\mu\text{M}$	Hill coefficient
Wild type	15 $\pm$ 1.0	2.4 $\pm$ 0.3
H-C-C	9.9 $\pm$ 2.0	1.3 $\pm$ 0.2
H-C-C plus 20 $\mu\text{M}$ Cd <sup>2+</sup>	3.2 $\pm$ 0.2	1.3 $\pm$ 0.1
C-C-C	5.7 $\pm$ 0.5	1.8 $\pm$ 0.2
C-C-C plus 20 $\mu\text{M}$ Cd <sup>2+</sup>	3.7 $\pm$ 0.2	2.6 $\pm$ 0.3
H-C-C concatamer B (1 subunit)	5.6 $\pm$ 0.1	1.4 $\pm$ 0.1
H-C-C concatamer C (2 subunits)	5.7 $\pm$ 0.9	1.4 $\pm$ 0.2
H-C-C concatamer D (3 subunits)	6.7 $\pm$ 1.3	0.9 $\pm$ 0.1
Intersubunit concatamer E	11.5 $\pm$ 0.4	1.9 $\pm$ 0.1
Intersubunit concatamer F	11.9 $\pm$ 1.6	1.6 $\pm$ 0.3
Intersubunit concatamer G	13.9 $\pm$ 0.9	1.8 $\pm$ 0.2

Concentration–response relationships for activation by ATP were generated from three to seven cells as described in *Methods*. Values for the wild-type channel are from Li et al. (1).

1. Li M, Chang TH, Silberberg SD, Swartz KJ (2008) Gating the pore of P2X receptor channels. *Nat Neurosci* 11(8):883–887.